KANSAS GEOLOGICAL SURVEY
OPEN-FILE REPORT 2003-81

Pfsim.xls: A DYNAMIC EXCEL WORKBOOK FOR FORWARD-MODELING OF LOG RESPONSES FROM MONTE CARLO SIMULATIONS OF SANDSTONE HYDROCARBON RESERVOIRS

by

John H. Doveton

Disclaimer

The Kansas Geological Survey does not guarantee this document to be free from errors or inaccuracies and disclaims any responsibility or liability for interpretations based on data used in the production of this document or decisions based thereon. This report is intended to make results of research available at the earliest possible date, but is not intended to constitute final or formal publications.

Kansas Geological Survey
1930 Constant Avenue
University of Kansas
Lawrence, KS 66047-3726

pfsim.xls: A DYNAMIC EXCEL WORKBOOK FOR FORWARD-MODELING OF LOG RESPONSES FROM MONTE CARLO SIMULATIONS OF SANDSTONE HYDROCARBON RESERVOIRS

John H. Doveton
Energy Research Section,
Kansas Geological Survey

December, 2003

Open-File Report 2003- 81

Introduction

Conventional log analysis applies the Archie equation to wireline resistivity and porosity measurements in the computation of a water saturations in potential reservoir sections. The process is commonly (and maybe appropriately) termed "log interpretation", both because of the inherent uncertainties regarding the true values of the parameters in the Archie equation and the need to reconcile the calculated fluid distribution with the physics of a buoyant hydrocarbon column in its penetration of the pore structure of successive sedimentary units in a sandstone reservoir. The reasoning is an inverse approach in which log responses are used to deduce the rock properties that control them. Alternatively, "forward-modeling" can be applied to predict log responses, based on rock properties and capillary pressure measurements, and a comparison made between predictions and log curves in a search for the optimal reservoir model.

Forward-modeling software can be written as an EXCEL spreadsheet, using standard functions rather than specialized macros, as demonstrated by this report and the workbook on the attached diskette. The procedure follows the following steps (see Fig. 1):
(1) the identification of petrofacies to characterize rock units in terms of common associations of porosity, permeability, and fluid saturation:
(2) the construction of a transition probability matrix of the petrofacies to be used in creating a stratigraphic column of the petrofacies sequence as a Markov chain realization;
(3) the assignation of a representative porosity to each zone of the model sequence according to its petrofacies;
(4) the estimation of the permeability of each zone, based on its petrofacies and porosity;
(5) the prediction of the water saturation of each zone, using Pittman equation calibrations with height above free-water level (the base of the simulated section),and the zone porosity and permeability;
(6) the generation of the resistivity log curve for the simulated section, as a forward-modeling application of the Archie equation;
(7) the display of a Pickett plot of resistivity and porosity as an expectation of a log pattern to be compared with observed crossplotted logs.

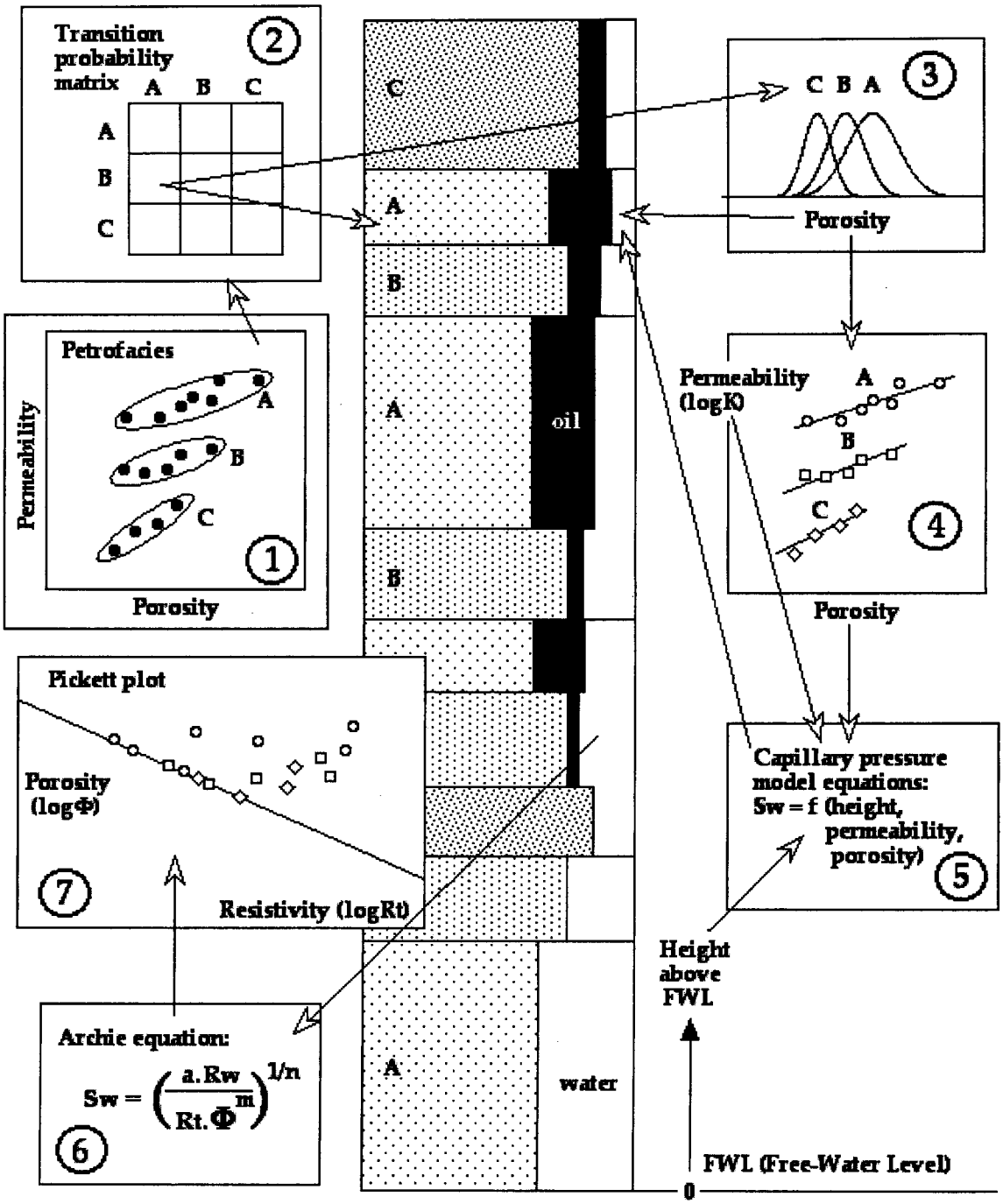

Figure 1. Flow diagram of operational steps (numbered in order) to simulate a sandstone reservoir and compute its wireline log responses.

1. Petrofacies identification

There are numerous ways to subdivide sandstones into facies, based on mineralogy, bedding structures, paleontology and other characteristics. However, the purpose of conventional geological facies is a classification that reflects the genesis of the sandstone and/or its diagenetic history. By contrast, effective petrofacies subdivision is morphological, rather than genetic, and should reflect the pore space of the rock in terms of volume, pore body and pore throat size distributions, geometry and connectivity. These factors control reservoir quality and differentiate flow units within a reservoir. Criteria to define petrofacies in sandstones may be based on petrographic observations of grain size, sorting, and other textural measures and/or petrophysical measures of porosity and permeability.

The example data set of this report used for demonstrating the modeling methodology is drawn from (unpublished) measurements of porosity, permeability, and grain-size of Simpson Sandstone core samples from Stafford County, Kansas by Alan Byrnes. Byrnes subdivided the sample set between medium-fine grained sandstone (petrofacies A), very fine-grained sandstone (petrofacies B), and very fine-grained/ silty sandstone (petrofacies C).The crossplot of porosity and permeabilty of these samples (Figure 2 and pfsim.xls, worksheet 'petrofacies') shows that the grain-size petrofacies subdivision is reflected by systematic and distinctive petrophysical trends, with increasing grain-size matched by higher permeability, as would be expected for the decrease in internal specific area. So, although the petrofacies were defined petrographically, the classification captures useful petrophysical distinctions between Simpson Sandstone poretype families. The measurement data and their statistical averages are shown in Figure 3 (and pfsim.xls, worksheet 'petrofacies'),

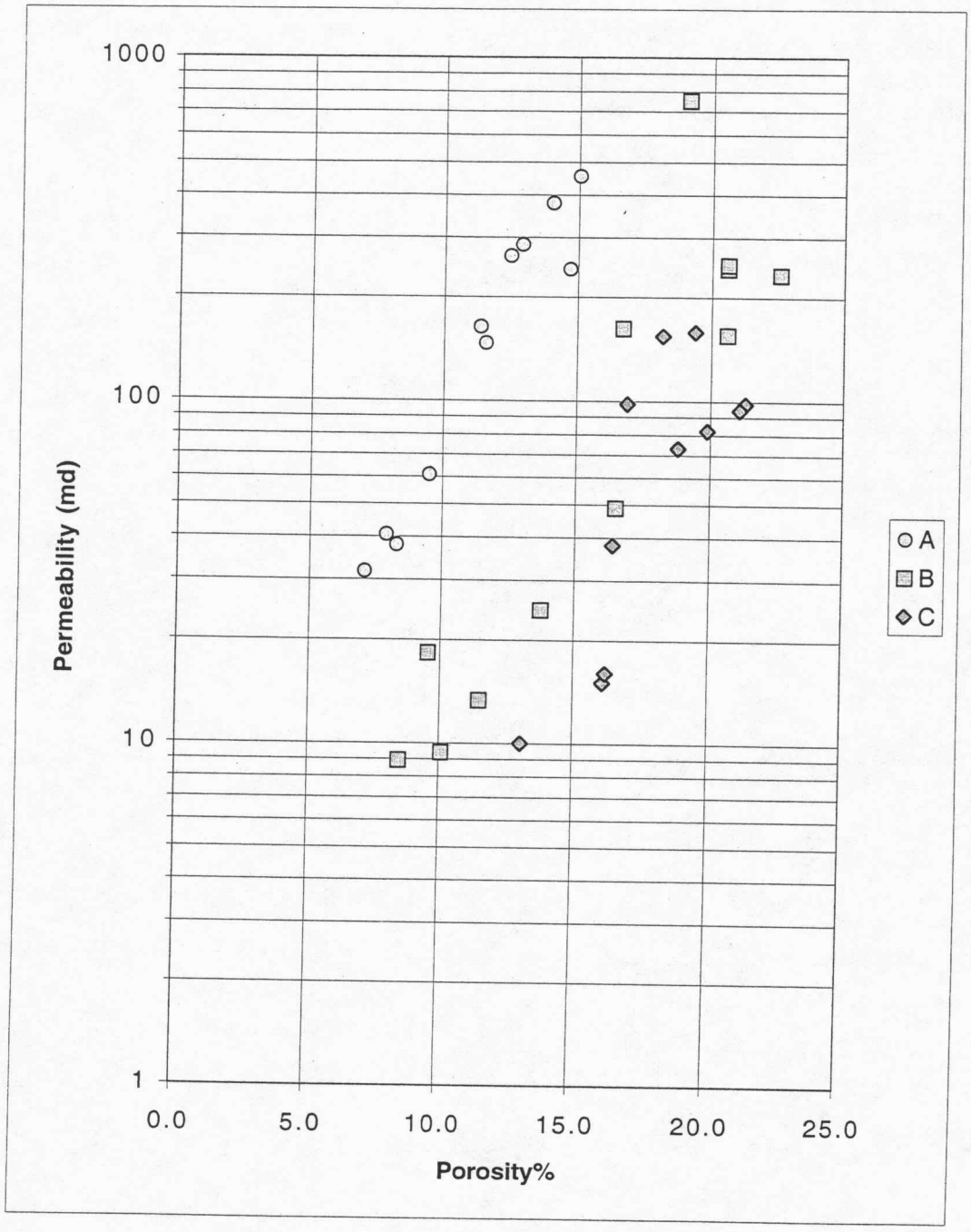

Figure 2. Crossplot of porosity and permeabilty of Simpson Sandstone core samples from Stafford County, Kansas measured by Alan Byrnes :medium-fine grained sandstone (petrofacies A), very fine-grained sandstone (petrofacies B), and very fine-grained/ silty sandstone (petrofacies C).

Petrofacies: porosity versus permeability
Simpson Sandstone sorted by grain size and basic lithofacies

ID#	% Porosity	Permeability md med-fn ss A	vfn ss B	/fn-slty ss C
18	15.0	455		
19	12.9	287		
20	14.0	379		
58	11.6	147		
59	14.7	243		
60	12.5	265		
61	11.4	164		
62	9.5	61.0		
63	7.1	31.7		
64	8.3	38.0		
65	7.9	40.7		
1	8.5		8.92	
2	11.5		13.3	
3	10.1		9.41	
4	13.8		24.5	
5	9.6		18.2	
43	20.6		155.0	
44	22.6		233	
45	20.6		243	
46	20.6		249	
47	16.5		48.8	
56	16.7		162	
57	19.1		751	
31	18.2			154
32	19.4			158
33	21.3			98.0
34	21.1			94.0
35	19.9			82.0
36	16.9			98.0
37	18.8			73.0
38	16.4			38.0
39	16.1			15.0
40	16.2			16.0
41	13.1			10.0

Petrofacies A mean values

Porosity	Permeability
11.4	132.9

Petrofacies B mean values

Porosity	Permeability
15.8	65.7

Petrofacies C mean values

Porosity	Permeability
17.9	54.3

Figure 3. Summary of porosity and permeabilty measurements of Simpson Sandstone core samples from Stafford County, Kansas (data from Alan Byrnes) :medium-fine grained sandstone (petrofacies A), very fine-grained sandstone (petrofacies B), and very fine-grained/ silty sandstone (petrofacies C).

2. Petrofacies sequence simulation

A Markov chain succession of petrofacies units can be generated as a Monte Carlo simulation, by the use of a random number generator in conjunction with a transition probability matrix. The general structure of the transition probability matrix takes the form of a probability table, where each row is matched with a petrofacies at some time increment and the cells contain the probability that the sequence will be in the petrofacies matched with the column at the following time increment. In this application, "time" is transformed to depth and an increment of 0.5 feet was chosen to match standard digital log sampling frequency. The probabilities in the matrix diagonal cells control the thickness distribution of each petrofacies.

In the workbook pfsim.xls, the transition probability matrix is under the control of the user. By changing the matrix input values, sequences with fining-upwards or coarsening-upwards trends can be generated and petrofacies modeled with varying thicknesses. The structure of the sequence generator is shown in Figure 4 (and pfsim.xls, worksheet 'markov'). The user enters values in the transitional probability matrix, with the condition that the probabilities in each row sum to unity, and an initial state of either A, B, or C. The sheet then generates a sequence of states as an ordered set from a an initial time of zero to 100 units, using an EXCEL random number generator of RAND() in conjunction with a look-up table generated from the transition probability matrix. The time series is then inverted to a depth sequence of petrofacies, where initial petrofacies is set at the Free-Water Level (FWL) of the reservoir and the successive incremental states are scaled at half-foot intervals above the FWL. The top of the succession in the workbook is at 50 feet above FWL. By this choice of range, the final model will scaled to represent transition zones and the lower parts of reservoirs that are at "irreducible" water saturation. The limitation in scale is appropriate for Kansas applications, but is also dictated by the poorer performance of Pittman equations in modeling saturations above the transition zone.

MARKOV CHAIN SEQUENCE SIMULATOR

Initial state (A, B, or C) = C

Transition probability matrix

P=

	A	B	C
A	0.8	0.2	0
B	0.1	0.7	0.2
C	0.1	0.3	0.6

Lookup table

	A	B	C	Z
A	0	0.8	1	1
B	0	0.1	0.8	1
C	0	0.1	0.4	1

t	X(t)	RAND	X(t+1)					Height(ft)	
0	C	0.071	A	0	0.1	0.4	1	50	B
1	A	0.499	A	0	0.8	1	1	49.5	B
2	A	0.167	A	0	0.8	1	1	49	B
3	A	0.072	A	0	0.8	1	1	48.5	B
4	A	0.795	A	0	0.8	1	1	48	B
5	A	0.738	A	0	0.8	1	1	47.5	B
6	A	0.068	A	0	0.8	1	1	47	A
7	A	0.135	A	0	0.8	1	1	46.5	A
8	A	0.221	A	0	0.8	1	1	46	B
9	A	0.274	A	0	0.8	1	1	45.5	B
10	A	0.798	A	0	0.8	1	1	45	B
11	A	0.943	B	0	0.8	1	1	44.5	B
12	B	0.781	B	0	0.1	0.8	1	44	B
13	B	0.556	B	0	0.1	0.8	1	43.5	B
14	B	0.165	B	0	0.1	0.8	1	43	B
15	B	0.686	B	0	0.1	0.8	1	42.5	A
16	B	0.051	A	0	0.1	0.8	1	42	B
17	A	0.6	A	0	0.8	1	1	41.5	C
18	A	0.074	A	0	0.8	1	1	41	B
19	A	0.435	A	0	0.8	1	1	40.5	B
20	A	0.904	B	0	0.8	1	1	40	B
21	B	0.57	B	0	0.1	0.8	1	39.5	B
22	B	0.614	B	0	0.1	0.8	1	39	B
23	B	0.583	B	0	0.1	0.8	1	38.5	B
24	B	0.507	B	0	0.1	0.8	1	38	B
25	B	0.973	C	0	0.1	0.8	1	37.5	A
26	C	0.46	C	0	0.1	0.4	1	37	A
27	C	0.262	B	0	0.1	0.4	1	36.5	C
28	B	0.658	B	0	0.1	0.8	1	36	C
29	B	0.769	B	0	0.1	0.8	1	35.5	C
30	B	0.5	B	0	0.1	0.8	1	35	C
31	B	0.438	B	0	0.1	0.8	1	34.5	B
32	B	0.789	B	0	0.1	0.8	1	34	A
33	B	0.286	B	0	0.1	0.8	1	33.5	A
34	B	0.637	B	0	0.1	0.8	1	33	B

Figure 4. The structure of the transition probability matrix and Markov chain sequence generator on pfsim.xls, worksheet 'markov'.

3 .Allocation of pore volumes and 4. permeabilities to a simulated succession of petrofacies

At each depth increment of the simulation, the petrofacies is identified and a porosity assigned, using a random number to select a value based on the petrofacies mean value and standard deviation (summarized in Figure 5 and on. pfsim.xls, worksheet 'petrofacies'. By using the EXCEL function NORMSINV(RAND()), the random numbers conform closely to a normal distribution, which is used a the model to characterize the porosity distributions in the three petrofacies.

From a regression analysis of logarithmic permeability predicted from porosity (Figures 5 and 6; pfsim.xls, worksheet 'petrofacies'), parameters for the intercept (a) and the slope (b) of each petrofacies were applied in the prediction of a permeability for each increment in the simulation.

Petrofacies characterization
Mean and standard deviations of porosity
Regression analysis of log k = a+b*phi

ID#	Phi	k	log k
18	0.15042	454.514	2.657547
19	0.12932	286.979	2.457851
20	0.14041	378.64	2.578226
58	0.116	147	2.167317
59	0.147	243	2.385606
60	0.125	265	2.423246
61	0.114	164	2.214844
62	0.095	61	1.78533
63	0.071	31.7	1.501059
64	0.083	38	1.579784
65	0.079	40.7	1.609594
1	0.08479	8.91569	0.950155
2	0.11531	13.3326	1.124915
3	0.10092	9.41183	0.973674
4	0.1378	24.5016	1.389195
5	0.09561	18.2438	1.261115
43	0.206	155	2.190332
44	0.226	233	2.367356
45	0.206	243	2.385606
46	0.206	249	2.396199
47	0.165	48.8	1.68842
56	0.167	162	2.209515
57	0.191	751	2.87564
31	0.182	154	2.187521
32	0.194	158	2.198657
33	0.213	98	1.991226
34	0.211	94	1.973128
35	0.199	82	1.913814
36	0.169	98	1.991226
37	0.188	73	1.863323
38	0.164	38	1.579784
39	0.161	15	1.176091
40	0.162	16	1.20412
41	0.131	10	1

Petrofacies A	
Porosity	
mean	**sd**
0.114	0.028
a	**b**
0.4385	14.8274

Petrofacies B	
Porosity	
mean	**sd**
0.158	0.050
a	**b**
-0.0985	12.0928

Petrofacies C	
Porosity	
mean	**sd**
0.179	0.025
a	**b**
-0.7084	13.6126

Figure 5. Petrofacies statistics for porosity and permeability.

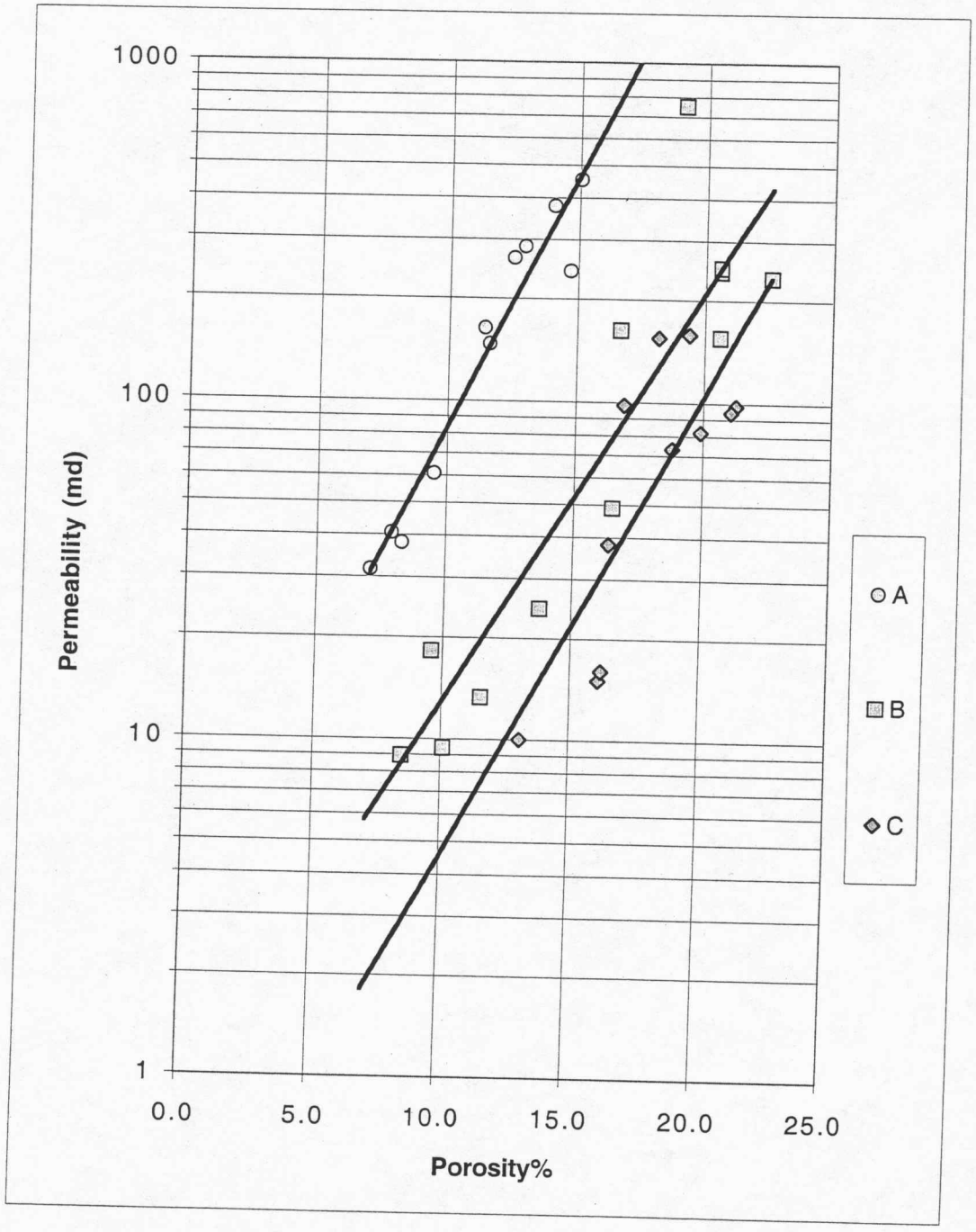

Figure 6. Permeability-porosity regression trends for petrofacies A, B, and C.

5. Pittman equation modeling of water saturations based on height above FWL, permeability, and porosity

Pittman (1992) made predictions of the radii of pore-throats penetrated over a range of mercury saturations from 10% to 75% in 5% increments. The measurements and statistical analysis were based on 202 sandstone samples from 14 formations, Ordovician to Tertiary in age, and with variation in composition and texture. Each equation was of the form:

$$\log(r_x) = A + B \cdot \log k + C \cdot \log \Phi$$

where r_X is the prediction of the radius of the smallest pore-throat penetrated when the sandstone is saturated by x% of mercury, k is the permeability of the sandstone in millidarcies, _ is the sandstone porosity in percent, and A, B, and C are constants determined by the regression analysis. The Pittman equation coefficients were used first to model capillary pressure curves based on the average porosity and permeability of the three petrofacies (Figure 7 and pfsim.xls, worksheet 'petrofacies'). The pore throat radius was converted to equivalent capillary pressure in a mercury/air system in units of psi, and then converted to equivalent height of oil column in feet, using a conversion number under user control.

Pittman (1992) noted that at the lower range of mercury saturation (10-35), the porosity term was not statistically significant and pore-throat radius could be predicted equally well by using permeability alone. Predictions in the range from 10 to 55% mercury saturation appeared to be the most reliable with correlation coefficients in excess of 0.90. Above 55% mercury, the regression fits declined progressively. Consequently the Pittman equations provide an adequate first-order model for sandstones, particularly in the transition zone, but predictions degrade at higher levels so that the simulation is best restricted to a limited interval above the FWL, and is fifty feet in pfsim.xls.

The Pittman equations are used in conjunction with the simulated succession by using the porosity and permeability at each level to compute a vector of expected heights above FWL that correspond to fixed increments of water saturation and then using the actual height above FWL to select the matching water saturation by an EXCEL look-up function as shown in Figure 8 (and pfsim.xls, worksheet 'markov').

Finally, the petrofacies assignments, porosities, and water saturations are combined together in a graphic profile of the simulated succession, ranging over a fifty-foot interval above the FWL (Figure 9 and pfsim.xls, worksheet 'markov').

PITTMAN'S EMPIRICAL EQUATIONS FOR SANDSTONES EXTENDED TO PREDICT HYDROCARBON COLUMN HEIGHT OVER A RANGE OF MERCURY SATURATIONS, BASED ON CORE POROSITY AND PERMEABILITY

	Porosity%	Permeability, md
A	11.4	132.9
B	15.8	65.7
C	17.9	54.3

PSI to hydrocarbon column conversion constant = 0.70

	Pore throat size (log r)				Height above FWL (feet)		
Hg%	A	B	C	Sw%	A	B	C
10	1.114	0.906	0.844	90	5.8	9.3	10.8
15	1.050	0.846	0.785	85	6.7	10.7	12.4
20	1.000	0.798	0.739	80	7.5	12.0	13.7
25	0.962	0.750	0.687	75	8.2	13.4	15.5
30	0.933	0.706	0.638	70	8.8	14.8	17.3
35	0.902	0.655	0.580	65	9.4	16.7	19.8
40	0.877	0.603	0.518	60	10.0	18.8	22.9
45	0.871	0.547	0.443	55	10.1	21.4	27.1
50	0.834	0.471	0.354	50	11.0	25.4	33.3
55	0.783	0.387	0.258	45	12.4	30.9	41.6
60	0.711	0.277	0.133	40	14.6	39.8	55.5
65	0.646	0.169	0.008	35	17.0	51.1	73.9
70	0.550	0.030	-0.147	30	21.2	70.3	105.8
75	0.398	-0.161	-0.353	25	30.1	109.1	170.0

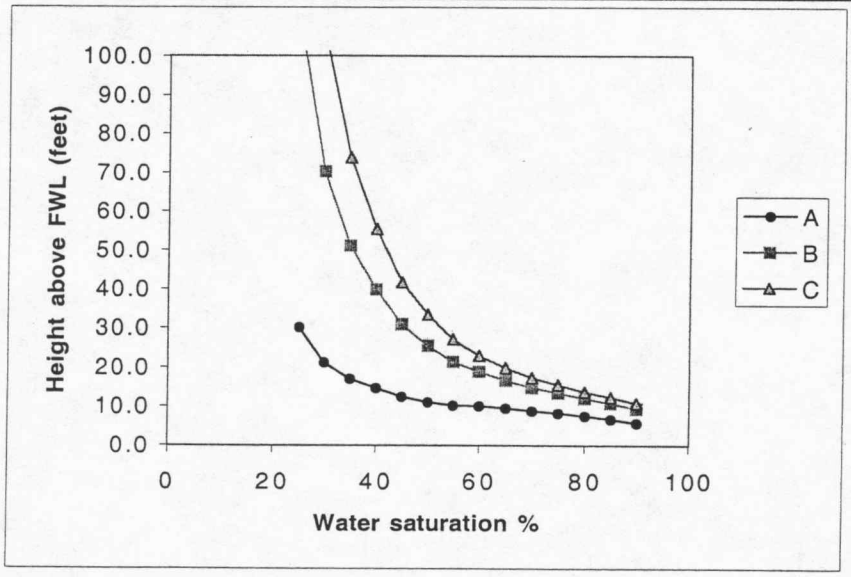

Figure 7. Use of the Pittman equation coefficients to model capillary pressure curves based on the average porosity and permeability of the three petrofacies.

PITTMAN EQUATIONS

Capillary pressure (psi) to height (feet) conversion = 0.7

Water saturation - height look-up table

Height	1	0.9	0.85	0.8	0.75	0.7	0.65	0.6	0.55	0.5	0.45	0.4	0.35	0.3	0.25	SW
50	0	12.9	15.1	17.1	19.2	21.2	23.7	26.2	28.8	33.1	38.7	48.2	57.9	73.5	106	0.4
49.5	0	22.7	27.6	32.5	36.1	39.3	42.6	44.3	42.8	44.5	46.2	51.5	51.3	52.6	61.5	0.45
49	0	4.62	5.16	5.59	6.23	6.86	7.73	8.92	10.7	13.3	17.1	23.3	33.3	52.4	92.5	0.35
48.5	0	5.74	6.46	7.06	7.87	8.69	9.8	11.3	13.3	16.4	20.8	27.9	38.7	58.7	100	0.35
48	0	27.1	33.5	40.3	44.3	47.5	50.1	49.8	43.8	42.3	40.6	41.8	37	33.1	34.1	0.7
47.5	0	3.62	4.01	4.3	4.77	5.25	5.91	6.85	8.3	10.4	13.7	18.8	27.7	45.2	83	0.3
47	0	8.84	10.5	12.1	13.1	14	14.8	15.1	14.3	14.7	15.4	17.1	17.7	19.4	24.3	0.25
46.5	0	7.55	8.87	10.1	11	11.8	12.5	13	12.7	13.4	14.4	16.4	17.9	20.7	27.3	0.25
46	0	26.7	33	39.7	43.7	46.9	49.6	49.5	44	42.7	41.3	42.9	38.4	34.8	36.3	0.75
45.5	0	9.15	10.5	11.7	13.1	14.5	16.3	18.4	21	25.1	30.5	39.4	50.8	70.4	110	0.4
45	0	13.9	16.3	18.6	20.8	23	25.6	28.3	30.6	35	40.4	49.8	58.7	73.1	103	0.45
44.5	0	5.77	6.5	7.1	7.92	8.74	9.86	11.3	13.4	16.5	20.9	28	38.8	58.9	100	0.35
44	0	4.72	5.28	5.72	6.37	7.02	7.92	9.13	10.9	13.6	17.5	23.7	33.8	53	93.3	0.35
43.5	0	8.68	9.95	11.1	12.4	13.7	15.4	17.4	20	23.9	29.3	38.1	49.5	69.3	109	0.4
43	0	18.2	21.6	25.1	28	30.7	33.9	36.4	37.6	41.2	45.4	53.5	58.5	66.6	86.1	0.5
42.5	0	6.47	7.54	8.52	9.3	9.93	10.6	11.2	11.2	12	13.3	15.4	17.5	21.1	29.1	0.25
42	0	12.3	14.3	16.2	18.1	20.1	22.4	25	27.5	31.9	37.5	47	57.1	73.6	107	0.45
41.5	0	7.24	8.31	9.25	10.3	11.2	12.4	13.8	15.2	17.6	21.1	26.5	33.5	45.4	69.6	0.35
41	0	7.53	8.57	9.47	10.6	11.7	13.2	15	17.4	21.1	26.2	34.4	45.8	66.1	107	0.4
40.5	0	6.17	6.97	7.64	8.53	9.42	10.6	12.2	14.3	17.5	22.1	29.5	40.6	60.8	102	0.4
40	0	12.4	14.4	16.3	18.2	20.2	22.6	25.1	27.7	32	37.6	47.1	57.2	73.6	107	0.45
39.5	0	10.9	12.7	14.2	15.9	17.6	19.7	22.1	24.8	29.1	34.7	44.1	54.9	72.9	109	0.45
39	0	11.5	13.4	15.1	16.9	18.7	20.9	23.3	26	30.3	35.9	45.4	55.9	73.3	109	0.45
38.5	0	11.7	13.6	15.4	17.2	19	21.3	23.8	26.4	30.7	36.3	45.8	56.3	73.4	108	0.45
38	0	1.95	2.11	2.22	2.44	2.66	2.98	3.48	4.3	5.5	7.46	10.5	16.5	29.4	58.8	0.3
37.5	0	4.37	5	5.54	6.04	6.46	6.96	7.47	7.81	8.71	10.1	12.3	15	20	30.2	0.25
37	0	5.96	6.91	7.78	8.49	9.07	9.73	10.3	10.4	11.3	12.6	14.8	17.1	21.1	29.7	0.25
36.5	0	3.17	3.52	3.8	4.18	4.54	5.03	5.7	6.62	8.05	10.2	13.6	19.3	30.3	53.7	0.3
36	0	6.05	6.89	7.62	8.44	9.22	10.2	11.4	12.8	15	18.2	23.3	30.3	42.6	67.7	0.35
35.5	0	1.84	2.01	2.12	2.32	2.5	2.76	3.14	3.72	4.6	6.04	8.2	12.3	20.9	39.9	0.3
35	0	5.06	5.72	6.28	6.95	7.58	8.41	9.43	10.7	12.7	15.7	20.3	27.1	39.4	64.6	0.35
34.5	0	14.9	17.5	20.1	22.4	24.7	27.5	30.2	32.4	36.6	41.8	51.1	59.2	72.2	99.8	0.55
34	0	5.36	6.19	6.92	7.56	8.08	8.68	9.23	9.44	10.4	11.7	14	16.5	20.9	30.2	0.25
33.5	0	3.92	4.46	4.91	5.36	5.73	6.18	6.66	7.03	7.91	9.27	11.3	14.2	19.3	29.8	0.25
33	0	13.4	15.6	17.8	19.9	21.9	24.5	27.1	29.6	33.9	39.4	48.9	58.3	73.4	105	0.55
32.5	0	7.01	7.96	8.76	9.79	10.8	12.2	13.9	16.2	19.7	24.6	32.6	43.9	64.3	106	0.45

Figure 8. Use of the Pittman equations in conjunction with the simulated succession by inputting the porosity and permeability at each level in the computation of a vector of expected heights above FWL that correspond to fixed increments of water saturation and then using the actual height above FWL to select the matching water saturation by an EXCEL look-up function.

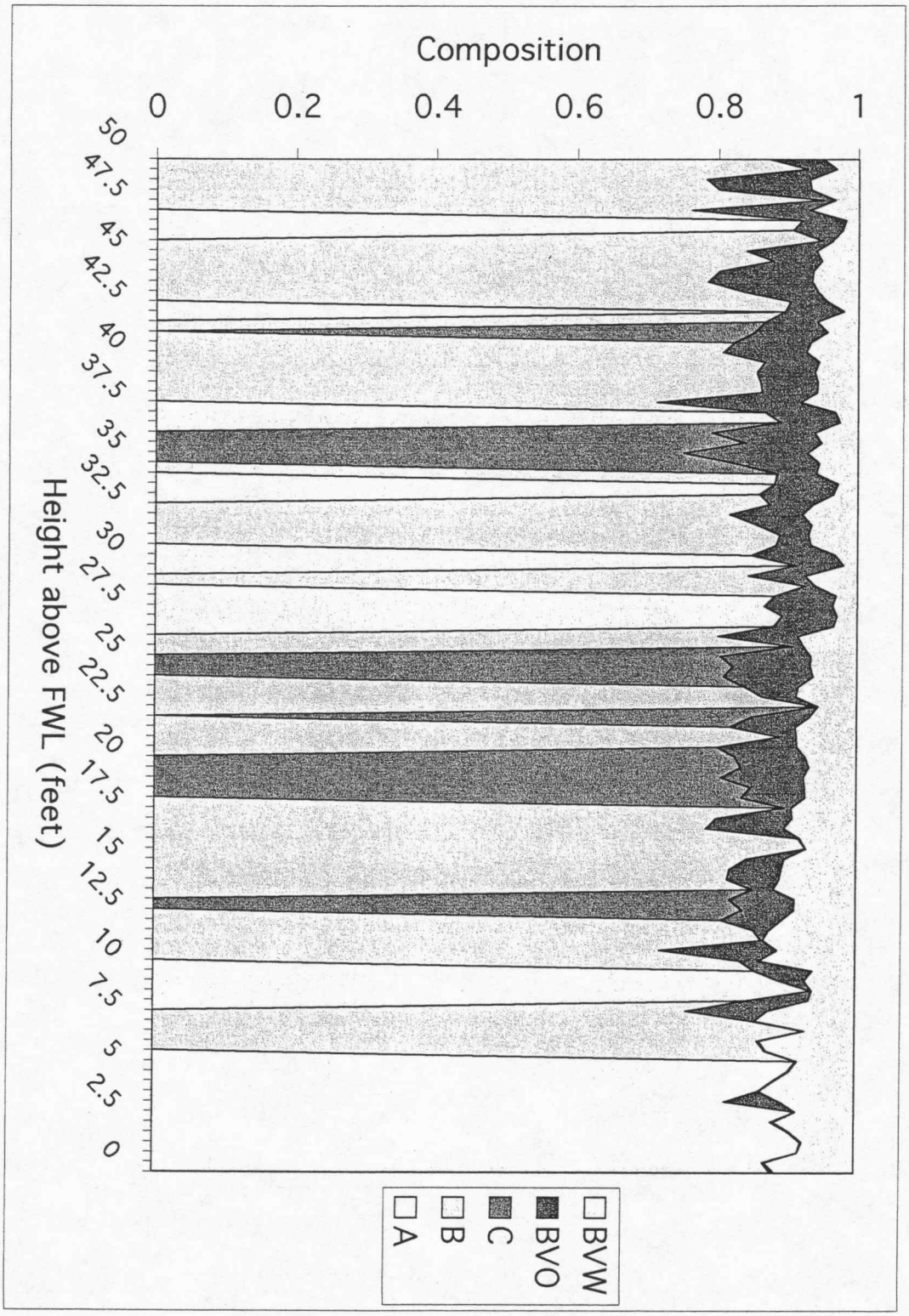

Figure 9. Compositional profile of simulation, graphed as petrofacies (A, B, or C), BVW (bulk-volume water), and BVO (bulk-volume oil).

6. Forward-modeling of resistivity curves and 7. generation of a Pickett plot

The Archie equation is applied to forward-model the resistivity log curve, using porosities and water saturations from the simulation. The values of the Archie equation parameters are selected by the user (Figure 10 and pfsim.xls, worksheet 'markov').

The porosity and resistivity values are then located on a Pickett plot (Figure 11 and pfsim.xls, worksheet 'markov') for evaluation in terms of the model and comparative work with real successions.

Conclusions

The software model presented in this report represents a first step in an integrated petrophysical evaluation, as a tool in forward-modeling of petrofacies to their expected log responses. In its current implementation, the workbook generates hypothetical successions, although they are controlled by the user's input of transition probabilities. However, future versions will be applied with real successions so that the workbook can be moved beyond a teaching tool to aid in the interpretation of Pickett plots from real log suites to predictive capabilities of FWL estimation and analysis of reservoir flow-unit architecture.

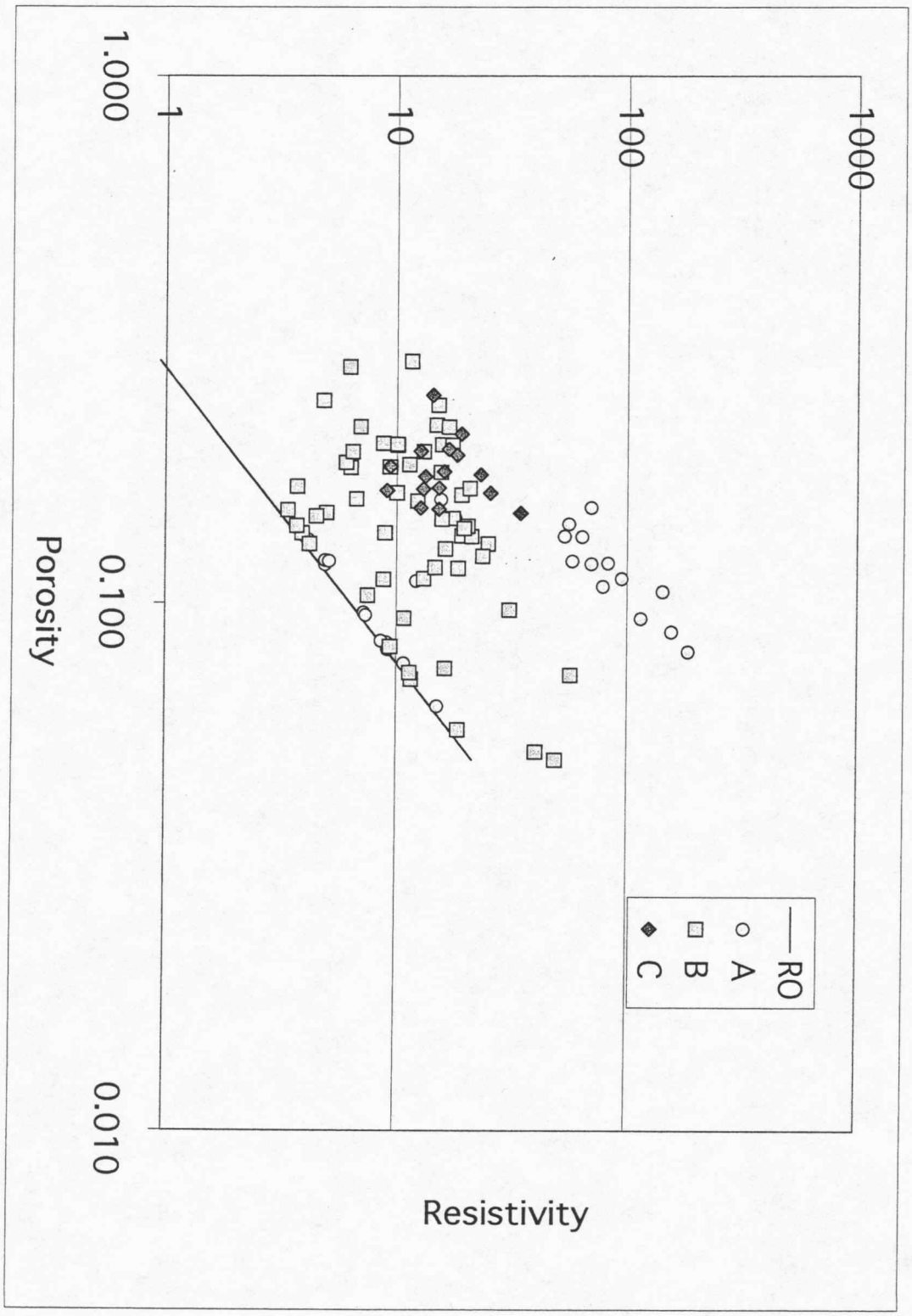

Figure 10. Pickett plot of resistivities and porosities from the simulation.